Thin electron-scale layers at the magnetopause

M. André,[1] A. Vaivads,[1] S. C. Buchert,[1] A. N. Fazakerley,[2] and A. Lahiff[2]

Received 9 July 2003; revised 15 September 2003; accepted 22 October 2003; published 4 February 2004.

[1] We use data from the four Cluster satellites to examine the microphysics of a thin electron-scale layer discovered on the magnetospheric side of the magnetopause. Here the ion and electron motions are decoupled in a layer about 20 km (a few electron scales) wide, including currents and strong electric fields. In this layer the electrons are $\mathbf{E} \times \mathbf{B}$ drifting with the ions as a background, and the region can be described by Hall MHD physics. A unique identification of the source of the thin layer is not possible, but our observations are consistent with recent simulations showing thin layers associated with the separatrix extending far away from a reconnection diffusion region. *INDEX TERMS:* 2712 Magnetospheric Physics: Electric fields (2411); 2724 Magnetospheric Physics: Magnetopause, cusp, and boundary layers; 7835 Space Plasma Physics: Magnetic reconnection. **Citation:** André, M., A. Vaivads, S. C. Buchert, A. N. Fazakerley, and A. Lahiff (2004), Thin electron-scale layers at the magnetopause, *Geophys. Res. Lett.*, *31*, L03803, doi:10.1029/2003GL018137.

1. Introduction

[2] The magnetopause is a complex boundary between the magnetosphere and the shocked solar wind. Previous single satellite missions could determine that the magnetopause current layer is often a few hundred km thick. Here the ion gyroradius ρ_i and the ion skindepth c/ω_i (speed of light/ion plasma frequency) are typically about hundred km, making the width of the magnetopause current layer a few ion scales. It was also clear that structures including waves and strong electric fields could occur on much smaller scales [*Cattell et al.*, 1995]. However, with a single spacecraft it is hard to determine whether a structure that is observed for a short time during a magnetopause crossing is due to an extended and rather steady layer, or a short burst of activity limited in both space and time.

[3] Solar wind particles, energy and momentum can be transferred across the magnetopause to the magnetosphere. So-called magnetic reconnection is believed to control much of this transfer. Observations of ion beams (jets) far away from the implied reconnection site are consistent with this scenario [*Phan et al.*, 2000]. The reconnection site, the so-called diffusion region where the ion and electron motions are decoupled, is much smaller than the regions where the resulting plasma acceleration can be seen. On a few occasions, spacecraft are believed to have directly observed some of the microphysics associated with reconnection [*Mozer et al.*, 2002; *Øieroset et al.*, 2001; *Deng and Matsumoto*, 2001]. The importance of transport across the magnetopause has recently inspired several theoretical and numerical studies of the microphysics at this boundary [*Rogers et al.*, 2000; *Shay et al.*, 2001; *Drake et al.*, 2003]. The point of this letter is to use data from the four Cluster satellites to examine the microphysics of a thin layer discovered on the magnetospheric side of the magnetopause. Here the ion and electron motions are decoupled in a layer about 20 km wide (a few electron scales) including currents and strong electric fields. Recent simulations [*Shay et al.*, 2001; *Rogers et al.*, 2000] show thin layers associated with the separatrix extending far away from a reconnection diffusion region. The cause of the thin layers we observe can not be uniquely identified, but our observations are consistent with the layers found in simulations.

2. Observations

[4] Cluster is a four-satellite mission with unique capabilities to study the outer boundaries of the magnetosphere. We investigate in detail data from the EFW double-probe electric field and wave instrument with two pairs of probes in the spin plane of each satellite, the FGM fluxgate magnetometer and the PEACE electron instrument, see *Escoubet et al.* [2001] and references therein.

[5] On February 6, 2002, around 0800 UT the Cluster satellites were at (4.6, 5.7, 8.5) R_e (GSE), i.e., in the high latitude afternoon magnetosphere at around 14 MLT. The spacecraft were approximately in a tetrahedron formation, with separation distances of about 100 km. The magnetopause passed the spacecraft formation several times. At about 0812 UT the PEACE electron instrument observations show a transition from electrons with energies of about one keV together with field-aligned 100 eV electrons, to a more isotropic 100 eV electron distribution with higher density. Also, the CIS ion instrument shows a transition from ions with energies mainly above 10 keV, to ions at one keV (not shown). Thus, particle observations are consistent with an outbound crossing of the magnetopause from the magnetosphere to the magnetosheath. At the magnetopause the proton inertial length is 190 km (density n = 1.5 cm^{-3}, estimated from the spacecraft potential), the proton gyroradius (1 keV) 90 km, the electron gyroradius (200 eV) 1 km, and the electron inertial length is 4 km. Figure 1 shows details of the field observations from this crossing.

[6] Panel a of Figure 1 shows the density estimated from the spacecraft potential (5 samples/s) [*Pedersen et al.*, 2001]. Assuming that the magnetopause locally is flat and that the magnetopause velocity is constant and normal to the boundary, the velocity can be estimated by timing some characteristic feature passing all satellites. We use the density increase in panel a. In Figure 1 the data of

[1]Swedish Institute of Space Physics, Uppsala, Sweden.
[2]Mullard Space Science Laboratory, University College London, United Kingdom.

0094-8276/04/2003GL018137

satellites 2, 3 and 4 have been shifted 0.19, 0.72 and −0.17 seconds respectively, so that the observations of the density gradient are aligned. The inferred velocity is 105(−0.76, −0.35, −0,54) km/s (GSE). The density observations are consistent with a crossing from the low density magnetosphere going out towards the higher density magnetosheath 0812:00 UT. There is also a density decrease at 0811:57.5–0811:59.0 UT in Figure 1. The next three panels show the magnetic field **B** (67 samples/s); B_L (component along the average B direction, panel d), B_N (normal to the magnetopause, b), B_M ($B_N \times B_L$, c). Approximately, perturbations in B_M and B_L correspond to field-aligned and perpendicular currents, respectively, while a changing B_N indicates that the current sheet is not completely flat and aligned with the magnetopause plane. The large-scale magnetopause current can be seen as a change in B_M and B_L after 0811:59 UT. We concentrate on a thinner current sheet indicated by **B** perturbations before 0811:58. Panels e-h show two components, approximately GSE X and Y, of the electric field **E** (450 samples/s, with a 180 Hz low-pass filter). Approximately 0811:57.5–0812:00 UT, coinciding with the density decrease, all spacecraft observe a quasi-static E-field corresponding to an $\mathbf{E} \times \mathbf{B}$ drift of about 200 km/s (along the magnetopause towards afternoon sector). Intense E-fields up to and above 50 mV/m are observed by satellite 1 and 4 at 0811:57.6–57.8 UT, coinciding with perturbations in B_M and B_L. On satellite 1 only one EFW probe-pair is operational during this event. Due to the phase of the 4 s satellite spin, E-fields in the Y direction could not be observed during this 0.2 s period. On satellite 2 and 3 E-fields up to 20 mV/m are observed during the same 0.2 s period, together with other strong emissions up to a second before this interval. Our observations are consistent with a thin layer of current and strong electric fields during 0.2 s at 0811:57.6–57.8 UT, i.e., with a 20 km wide layer (a few times the electron scale) in the magnetopause frame.

[7] In order to investigate the thin layer in detail we use the time-stationary form of the electron momentum equation written as a generalized Ohm's law

$$\mathbf{E} = \frac{1}{ne}\mathbf{j} \times \mathbf{B} - \frac{1}{ne}\nabla \mathbf{p}_e - \mathbf{u}_i \times \mathbf{B} - \frac{m_e}{e}\mathbf{u}_e \cdot \nabla \mathbf{u}_e \qquad (1)$$

[8] In the following we concentrate on the direction perpendicular to the magnetic field. Then the electric field **E**, the $\frac{1}{ne}\mathbf{j} \times \mathbf{B}$ Hall term, and the electron pressure gradient term (neglecting off-diagonal terms of the $\mathbf{p}_e$ tensor) can be estimated from each spacecraft. Figure 2 shows details of the thin layer detected by spacecraft 4. The display covers 2.5 seconds of one 4-second satellite spin. Panels a and b show electron data from two sectors of the PEACE detector. The direction of the detector sectors change as the satellite spins. At the thin layer (0811:57.4–57.6 UT, not time-shifted) panel a corresponds to a direction perpendicular to the magnetic field, while panel b shows field-aligned (Earthward) electrons. Panel c displays estimates of three terms in the generalized Ohms law: the electric field normal to the magnetopause plane (and normal to the magnetic field) which is the major E-field component, assuming $\mathbf{E} \cdot \mathbf{B} = 0$ with **B** about 45 degrees from the satellite spin plane; the

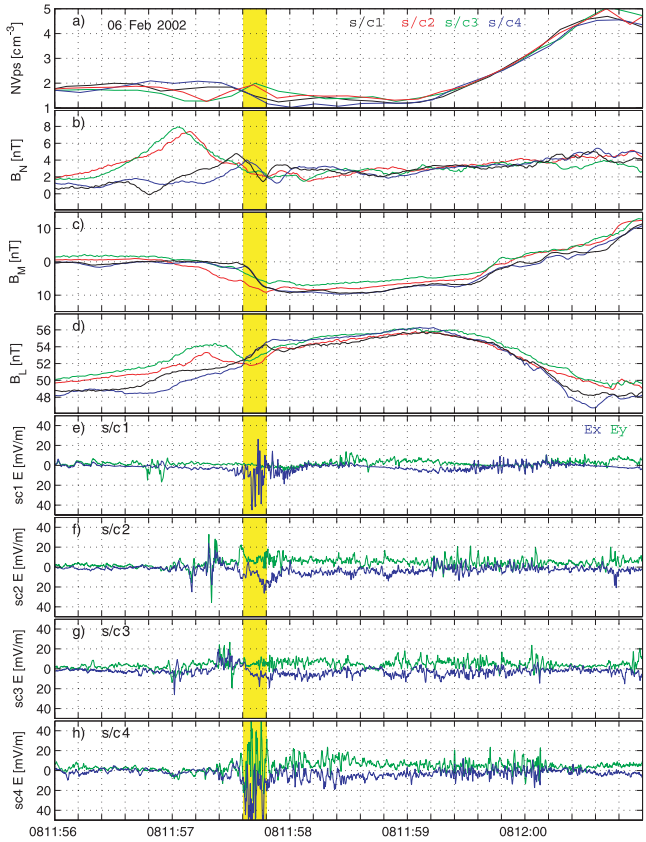

Figure 1. Density estimate, and **B** and **E** fields for a magnetopause crossing. Data are time shifted to align the density increase, using satellite 1 as reference. a) density for all spacecraft, b-d) B_N, B_M, B_L (see text), e-h) E sunward and duskward, approximately GSE X and Y, for each individual satellite. There is a thin layer at 0811:57.6–57.8 UT (indicated in yellow).

Hall term $\frac{1}{ne}\mathbf{j} \times \mathbf{B}$; and the pressure gradient $-\frac{1}{n}(T_e dn/dx)$ where x is the distance across the layer, assuming a constant electron temperature T_e of 150 eV. The lower panels show quantities used to derive the terms in panel c; the density n estimated from the satellite potential at 5 samples/s, and for comparison the same parameter sampled at 9 ksamples/s available since the EFW internal burst mode was triggered on this satellite (panel d); the total magnetic field amplitude (changes correspond to a perpendicular current, panel e) and the perpendicular and parallel components of the current, estimated from B-field perturbations on this single satellite and assuming that the current sheet is in the magnetopause plane (panel f). A 30 Hz low-pass filter has been applied to the observed **E**-field for comparison with the estimated currents. These observations from spacecraft 4 indicate a 20 km thin current layer where $\mathbf{E} \approx \frac{1}{ne}\mathbf{j} \times \mathbf{B}$, while the electron pressure gradient term is much smaller.

[9] The two last terms on the right-hand side of equation (1) can not easily be estimated directly from observations. The term $\mathbf{u}_i \times \mathbf{B}$, where $\mathbf{u}_i$ is the ion velocity, is hard to estimate from particle observations during a period much shorter than one satellite spin. A reasonable upper limit is

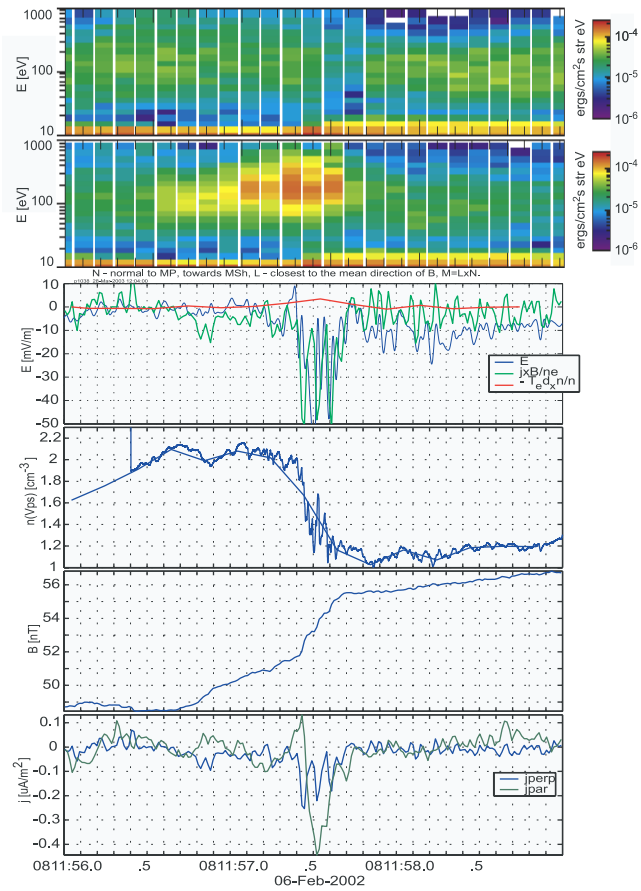

Figure 2. Electron, field and density data from satellite 4. a and b) Electron energy flux from two PEACE instrument sectors (ergs/cm^2 s sr eV), in the middle of the time interval corresponding to perpendicular and parallel (Earthward particles) directions, respectively, c) three terms in the generalized Ohms law derived from observations, d) density estimate at two sampling rates, e) magnetic field amplitude, f) field-aligned and perpendicular current.

10 mV/m obtained by comparing with the quasi-static E-field 0811:58–0812:00 UT. Also the last term, describing electron inertia, is hard to estimate. Taking 100 km/s (the large-scale $\mathbf{E} \times \mathbf{B}$ drift) as a typical value for u_e, and from comparing observations by different spacecraft taking 100 km to be a minimum scale-length of $\mathbf{u}_e$ along the thin layer gives an upper limit of about 10 mV/m. Thus none of the two last terms of equation (1) are likely to dominate the observed E-field, but some contribution can not immediately be discarded. Also, the terms including $\mathbf{p}_e$ and $\mathbf{u}_e \cdot \nabla \mathbf{u}_e$ are at electron scales candidates for producing a significant parallel electric field. This E-field component is likely to be much smaller than the perpendicular electric field, can not be reliably estimated for this event, and is not discussed in detail.

[10] The agreement between $\mathbf{E}$ and $\frac{1}{ne}\,\mathbf{j} \times \mathbf{B}$ is very good in the thin layer (Figure 2c) and all other terms in equation (1) are likely to be much smaller. In other words, the thin layer includes a parallel current carried by ~150 eV electrons. These electrons are also $\mathbf{E} \times \mathbf{B}$ drifting with the ions as a background, consistent with the observed E-field and the perpendicular current.

[11] Figure 3 gives some details of the thin layer for all four satellites. The density estimates in the upper panel are identical to panel a of Figure 1, including time shifts. Panels b-e show the observed $\mathbf{E}$, $\frac{1}{ne}\,\mathbf{j} \times \mathbf{B}$ filtered as in Figure 2, and $-\frac{1}{n}(T_e dn/dx)$ terms for satellites 1–4. All four spacecraft show a thin layer at 0811:57.6–57.8 UT with E-fields of 20 to above 50 mV/m and $\mathbf{E} \approx \frac{1}{ne}\,\mathbf{j} \times \mathbf{B}$, with a much smaller electron pressure gradient term. Since satellite 1 only has one operational probe-pair, the E-field in panel b is likely to be underestimated. The large Hall terms for satellites 2 and 3 at 0811:57.0–57.6 coincide with electric fields at higher frequencies (Figure 1) removed by our filtering. There is a potential drop across the thin layer, from about 400 V (satellite 4, E-field toward the magnetosphere) to about 100 V (satellite 3). As for Figure 2, data are consistent with a 20 km wide layer with a field-aligned current carried by electrons, and also with an electron $\mathbf{E} \times \mathbf{B}$ drift consistent with the observed E-field and perpendicular current.

[12] Several features in our data clearly show that we are observing a thin electron-scale layer, and not only a localized phenomenon. Currents and enhanced E-fields are observed on all spacecraft, and $\mathbf{E} \approx \frac{1}{ne}\,\mathbf{j} \times \mathbf{B}$ on all spacecraft, consistent with a thin layer essentially in the magnetopause plane. Also, large-scale $\mathbf{E}$ and particle features change at this thin layer. A quasi-static electric field is

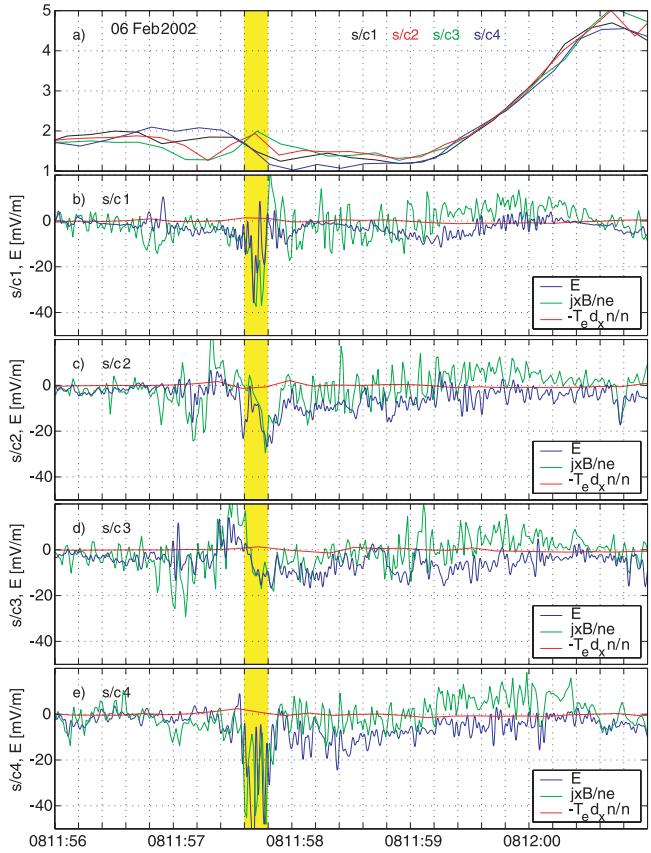

Figure 3. a) density estimate for all spacecraft, same as Figure 1, data are shifted to align the density increase, b-e) three terms in the generalized Ohms law derived from observations, for each individual satellite. There is a thin layer at 08:11:57:6–57:8 UT (indicated in yellow).

observed after the thin layer, but not before (Figure 1). On satellite 4 more electrons near one keV are present before the layer, as compared to later (Figure 2). Similar changes of the electron fluxes are observed on all spacecraft (not shown), consistent with the layer affecting particle populations extending far beyond the 100 km satellite separation.

[13] The time- and length-scales of phenomena in the thin layer can be estimated by comparing pairs of spacecraft. Satellite 1 and 4 are 100 km apart, but the perpendicular distance between the respective flux-tubes is only 20 km. The satellites observe E-fields of similar amplitude, but not identical fields. Since the satellites encounter the layer about 0.2 s apart, we conclude that the thin layer does not change much on lengths (times) of 20 km (0.2 s). Satellite 1 and 2 also cross the layer about 0.2 s apart, but the distance between flux-tubes is about 100 km. Here the observations vary more between spacecraft, satellite 2 observing somewhat smaller E-field in a slightly larger region. Satellite 1 and 3 encounter the layer about 0.8 s apart, and separated by 100 km across the B-field. The E-field on satellite 3 is smaller, and occurs in a somewhat broader region. In summary, the thin layer changes on length scales of 100 km and times of 1 s, i.e., on the ion scale, but is likely to extend much further along the magnetopause, and exist for much longer time.

3. Results and Discussion

[14] We present data showing the existence of a thin layer with a width of a few electron scales (a few ρ_e or c/ω_e) with currents and strong electric fields on the magnetospheric side of the magnetopause. The current ($0.1-1$ μ A/m^2) is mainly carried by electrons with energies of about 100 eV and is mainly field-aligned but has a significant perpendicular component. In this layer $\mathbf{E} \approx \frac{1}{ne}\,\mathbf{j} \times \mathbf{B}$, i.e., the electrons are $\mathbf{E} \times \mathbf{B}$ drifting with the ions as a background, and the region can be described by Hall MHD physics. The electric field is mainly perpendicular to the magnetic field (and normal to the magnetopause) with a magnitude of 20–100 mV/m. The electric field includes a quasi-static component, a plateau in the power spectrum around the lower hybrid frequency near 20 Hz and broadband emissions reaching several hundred Hz, as discussed in a companion paper [*Vaivads et al.*, 2004]. The resulting potential drop is a few hundred V. The electric field and current can be identified to belong to a thin layer rather than a limited perturbation using observations by four satellites.

[15] Strong electric fields (a few to hundred mV/m) are found at most magnetopause crossings observed by Cluster. Not all these crossings have a thin electron-scale layer such as the one investigated in this letter. It is likely that a more planar magnetopause without much perturbation on the ion scale is more favorable for the existence of a thin layer [*André et al.*, 2001].

[16] The thin layers clearly show that currents, electric fields and Hall MHD physics can occur on the electron scale at the magnetopause. It is interesting to note that recent simulations [*Shay et al.*, 2001; *Rogers et al.*, 2000] predict both a density depletion with a width of the ion scale, and an electron-scale layer with a current, an electric field and Hall MHD physics, associated with the separatrix extending far away from the reconnection diffusion region. One possible interpretation of our observations is that the Cluster satellites cross such a separatrix far away from a reconnection diffusion region. We note that the solar wind direction (as detected by the ACE satellite, including a positive B_y component of a few nT) on February 6 is consistent with a reconnection site near the Cluster location in the afternoon high latitude sector. In addition, our observations are relevant for simulations of whistler and Alfvén wave activity at small scales associated with reconnection [*Rogers et al.*, 2001]. The theoretical prediction and subsequent detection by spacecraft of microphysical phenomena far away from the reconnection site would open new possibilities for detailed comparison between simulations and observations. Both simulations and multi-spacecraft observations are now at a stage when this should be seriously attempted.

[17] **Acknowledgments.** Data analysis by Rico Behlke and discussions with Tai Phan and Barrett Rogers are gratefully acknowledged. CIS ion data were kindly provided by H. Rème and J.-A. Sauvaud.

References

André, M., et al. (2001), Multi-spacecraft observations of broadband waves near the lower hybrid frequency at the earthward edge of the magnetopause, *Ann. Geophys.*, *19*, 1471–1481.

Cattell, C., J. Wygant, F. S. Mozer, T. Okada, K. Tsuruda, S. Kokubun, and T. Yamamoto (1995), ISEE 1 and Geotail observations of low-frequency waves at the magnetopause, *J. Geophys. Res.*, *100*(A7), 11,823–11,830.

Deng, X. H., and H. Matsumoto (2001), Rapid magnetic reconnection in the Earth's magnetosphere mediated by whistler waves, *Nature*, *410*, 557–560.

Drake, J. F., M. Swisdak, C. Cattell, M. A. Shay, B. N. Rogers, and A. Zeiler (2003), Formation of electron holes and particle energization during magnetic reconnection, *Science*, *299*, 873–877.

Escoubet, C. P., M. Fehringer, and M. Goldstein (2001), The cluster mission, *Ann. Geophys.*, *19*, 1197–1200.

Mozer, F. S., S. D. Bale, and T. D. Phan (2002), Evidence of diffusion regions at a subsolar magnetopause crossing, *Phys. Rev. Lett.*, *89*, 15,002–15,005.

Øieroset, M., T. D. Phan, M. Fujimoto, R. P. Lin, and R. P. Lepping (2001), In situ detection of collisionless reconnection in the Earth's magnetotail, *Nature*, *412*, 414–417.

Pedersen, A., et al. (2001), Four-point high resolution information on electron densities by the electric field experiments (EFW) on Cluster, *Ann. Geophys.*, *19*, 1483–1489.

Phan, T. D., et al. (2000), Extended magnetic reconnection at the Earth's magnetopause from detection of bi-directional jets, *Nature*, *404*, 848–850.

Rogers, B. N., J. F. Drake, and M. A. Shay (2000), The onset of turbulence in collisionless magnetic reconnection, *Geophys. Res. Lett.*, *27*(19), 3157–3160.

Rogers, B. N., R. E. Denton, J. F. Drake, and M. A. Shay (2001), Role of dispersive waves in collosionless magnetic reconnection, *Phys. Rev. Lett.*, *87*, 100–103.

Shay, M. A., J. F. Drake, B. N. Rogers, and R. E. Denton (2001), Alfvénic collisionless magnetic reconnection and the Hall term, *J. Geophys. Res.*, *106*(A3), 3759–3772.

Vaivads, A., M. André, S. C. Buchert, J.-E. Wahlund, A. N. Fazakerley, and N. Cornilleau-Wehrlin (2004), Cluster observations of lower hybrid turbulence within thin layers at the magnetopause, *Geophys. Res. Lett.*, *31*, L03804, doi:10.1029/2003GL018142.

M. André, A. Vaivads, and S. C. Buchert, Swedish Institute of Space Physics, Box 537, SE-751 21 Uppsala, Sweden. (ma@irfu.se)

A. N. Fazakerley and A. Lahiff, Mullard Space Science Laboratory, University College London, United Kingdom.